the survivorship and fecundity of other individuals, their intrinsic rates must become more and more equal. Loosely, we expect ecological equivalents to coexist only if their r's are relatively equal.

A symmetrical situation exists in row 4 of Table 1. If $\alpha \rightarrow 1$, it is necessary for $K_i \approx K_j$ for the species to coexist. That is, as two species distinguish one another less and less, their carrying capacities must become more and more equal for coexistence. Again we might loosely state that ecological equivalents can only coexist if their K's are relatively the same.

A somewhat paradoxical situation exists here, since coexistence of ecological equivalents requires on the one hand similar intrinsic rates (r's) and on the other hand similar carrying capacities (K's). Clearly we are dealing with two distinct concepts of ecological equivalents. Ecological equivalents in the sense of $\alpha \rightarrow 1$ implies that the received effects of competition are the same for both species. Ecological equivalents in the sense of $\beta \rightarrow 1$ implies that the imposed effects of competition are the same for both species.

Finally, suppose $\alpha_{ij} << \alpha_{ji}$, as summarized in row 3 of Table 1. This time nothing can be said about the values of r and β (the classic situation), but $K_j > K_i$ is necessary if coexistence is to be likely.

In summary, the textbook approach to competition theory has ignored a reasonable interpretation of the meaning of competition. This oversight has led to a somewhat restricted view of the role of competition in nature, including the widespread belief that the qualitative outcome of competition is not dependent on the values of the intrinsic rates of natural increase. The analysis presented here indicates that this is not, in fact, a general result, but stems from a limited interpretation of simple equations. When the notion of β-competition is introduced, r becomes important in determining the outcome of competition. Furthermore, it is possible to suggest a negative correlation between competitive ability and the intrinsic rate of natural increase for species coexisting in nature.

JOHN H. VANDERMEER
Department of Zoology, University of Michigan, Ann Arbor 48104

References and Notes

1. See any ecology text, such as J. M. Emlen, *Ecology: An Evolutionary Approach* (Addison-Wesley, Reading, Mass., 1973); R. E. Ricklefs, *Ecology* (Chiron, Portland, Ore., 1973); E. R. Pianka, *Evolutionary Ecology* (Harper & Row, New York, 1974).
2. R. W. May, *Stability and Complexity in Model Ecosystems* (Princeton Univ. Press, Princeton, N.J., 1973).
3. G. J. Gausse, *The Struggle for Existence* (Williams & Wilkins, Baltimore, 1934).
4. A. Blaquière, *Nonlinear System Analysis* (Academic Press, New York, 1966); R. Rosen, *Dynamical System Theory in Biology* (Wiley-Interscience, New York, 1970).
5. J. F. Riebesell, *Ecology* **55**, 183 (1974).
6. J. H. Vandermeer, *Am. Nat.* **104**, 73 (1970).
7. This report was prepared in consultation with D. Boucher, D. Culver, W. Durham, K. Frogner, L. Real, V. Sork, R. Westman, and the students of Zoology 457 at the University of Michigan.

19 November 1974; revised 5 February 1975

Alaskan Thermokarst Terrain and Possible Martian Analog

Abstract. *A first-order analog to martian fretted terrain has been recognized on enhanced, ERTS-1 (Earth Resources Technology Satellite) imagery of Alaskan Arctic thermokarst terrain. The Alaskan analog displays flat-floored valleys and intervalley uplands characteristic of fretted terrain. The thermokarst terrain has formed in a manner similar to one of the processes postulated for the development of the martian fretted terrain.*

Earlier investigators have discussed the possible occurrence and characteristics of subsurface ice on Mars in connection with the occurrence of chaotic and fretted terrains (*1, 2*). We have examined ERTS-1 (Earth Resources Technology Satellite) imagery of the area around the Ikpikpuk and Price rivers in northern Alaska and have recognized an Alaskan Arctic thermokarst terrain that appears to be a close analog to the martian fretted terrain identified in the imagery of Mariner 9.

Figure 1 is a Mariner 9, narrow-angle (camera B) frame illustrating the principal features of martian fretted terrain. It shows relatively smooth and flat lowlands with gentle undulations, several scattered craters of recent origin, and a few locally rough areas. The lowlands are bordered in general by abrupt arcuate escarpments 0.5 to 2.0 km in height. The total extent of fretted terrain is estimated to be approximately 4.75×10^6 km^2 (3 percent of the planet's surface) (*2*). One of the processes postulated for the development of fretted terrain is the collapse of upland, cratered terrain. A possible mode of origin suggested by several investigators is the degradation of massive ground ice. However, skeptics have questioned the possibility of sufficient quantities of massive subsurface ice and it has been pointed out that no terrestrial analogs are known (*2*).

Owing to a fortunate coincidence of low sun angle and a uniform snow cover, we have been able to recognize what appears to be a close terrestrial analog in the ERTS-1 multispectral imagery of an area separating the Arctic coastal plain from the foothills of the Brooks Range in northern Alaska. Snow cover masks the vegetation patterns and the numerous thaw lakes. Enhancement techniques highlight the relief (1 to 30 m) (*3*) existing between flat-floored thermokarst depressions and northeast-southwest trending, intervalley uplands.

Figure 2 is a 9500-km^2 portion of an ERTS-1 multispectral scanner (MSS), band 7, enhanced image (ID 1237-21353) of this area. A linear contrast stretch and geometric corrections identical to those done on the imagery of the Mariner 6, 7, and 9 missions were carried out by the Image Processing Laboratory (IPL) of the Jet Propulsion Laboratory (*4*). This processing was applied to images taken in MSS spectral bands 4 (0.5 to 0.6 μm), 5 (0.6 to 0.7 μm), 6 (0.7 to 0.8 μm), and 7 (0.8 to 1.1 μm). The contrast stretch was done to enhance the tonal differences of this uniformly high-albedo image. The geometric correction merely skewed the image to compensate for the earth's motion under the satellite during image acquisition. Subsequent inspection showed that the enhancement of band 7 gave the best rendition of this scene. Figure 3 is an enlarged portion of the thermokarst area in Fig. 2. This enlargement ($\times$ 4) facilitates comparison of some of the features common to the terrains shown in Figs. 1 and 2.

Terrestrial thermokarst topography consists of pits, basins, valleys, and closed depressions with small hummocks often containing lakes (*5*). This topography is characteristic of degrading permafrost areas with high subsurface ice contents; as the ice melts, the surface collapses. Local forms of thermokarst topography depend on the amounts and configuration of the subsurface ice and the balance between thermal, mechanical, and fluvial erosion. The slumping can occur along a slope or cliff by slope recession (*6*) and in flat areas by subsidence upon removal of subsurface ice. This slumping process is characterized by the retreat of steep, often nearly vertical, walls. The rate of retreat and the resulting slope pattern vary with the ice content of the original slope material. During backwearing the slumping sediment becomes saturated from the melting ground ice and flows downslope (*7*), producing the flat or slightly undulating lowlands. Water produced during the melting of subsurface ice could form rivulets or "stream" channels; it is possible that the streamlike valley in the lowlands (Fig. 1) might have formed by such a process.

The thermokarst topography shown in Figs. 2 and 3 has formed in the Meade River unit of the Pleistocene Gubik Formation (*8*). This formation consists of unconsolidated marine and nonmarine (alternating) sediments with variable ice content (*9*). A major portion of the subsurface ice occurs as "ice gneiss" or "disseminated ice" (*10*). Ice gneiss is characterized by alternating layers of ice in the stratigraphic column. Disseminated ice is more or less homogeneously distributed and commonly forms by the in situ freezing of pore water. In terrestrial permafrost, the subsurface ice contents range from 30 to 90 percent (by volume) (*11*). Degradation of the total volume of ice in the upper portion of the stratigraphic column commonly results in thermokarsts up to 40 m in depth (*12*). Subsurface ice commonly originates from

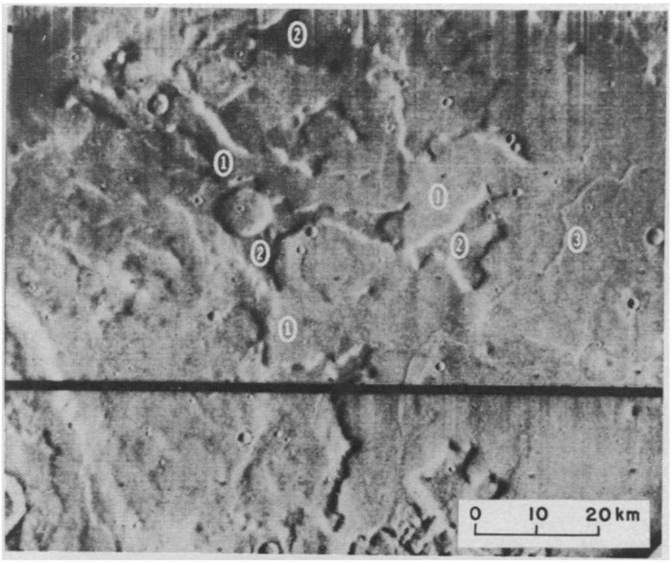

Fig. 1 (left). Narrow-angle, camera B frame of martian fretted terrain (MTVS 4233-91, DAS 08731179). Frame center, 44.0°N, 61.5°W; sun angle, 76.3°; scale as shown. North is to the top; *1*, lowlands; *2*, uplands; *3*, streamlike valley. Fig. 2 (lower left). Portion of a computer-enhanced, ERTS-1 band 7 image of the Alaskan Coastal Plain (ID 1237-21353). Frame center, 69.4°N, 153.3°W; sun angle, 19°; scale as shown. North is to the top; *1*, Ikpikpuk River; *2*, Price River; *3*, Brooks Range; *4*, thermokarst area. Fig. 3 (lower right). Enlargement (× 4) of the thermokarst area outlined in Fig. 2. North is to the top; *1*, uplands; *2*, irregularly shaped flat-floored pits, basins, and valleys.

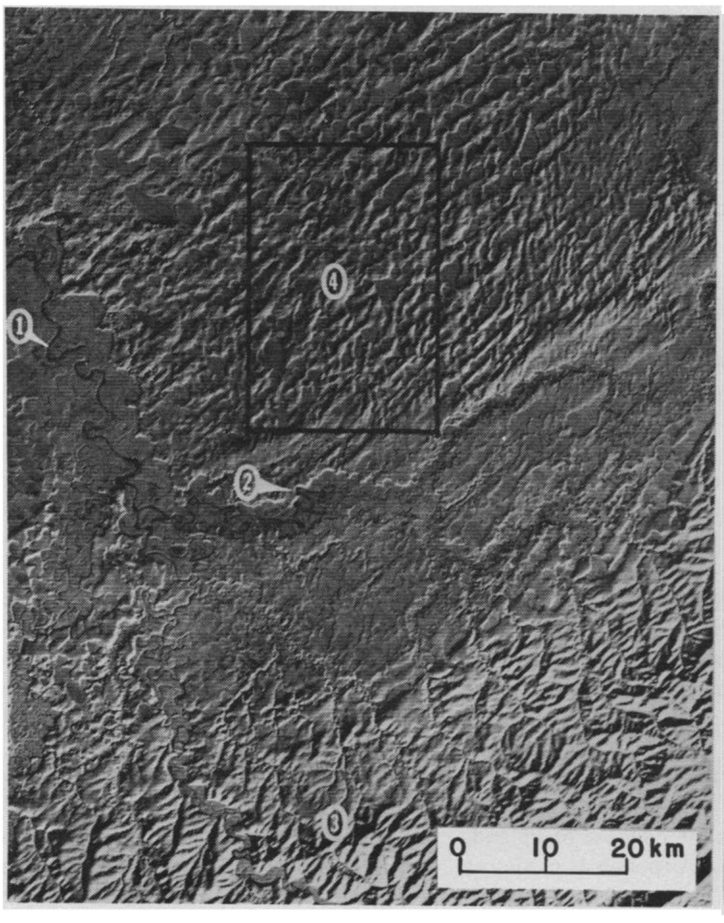

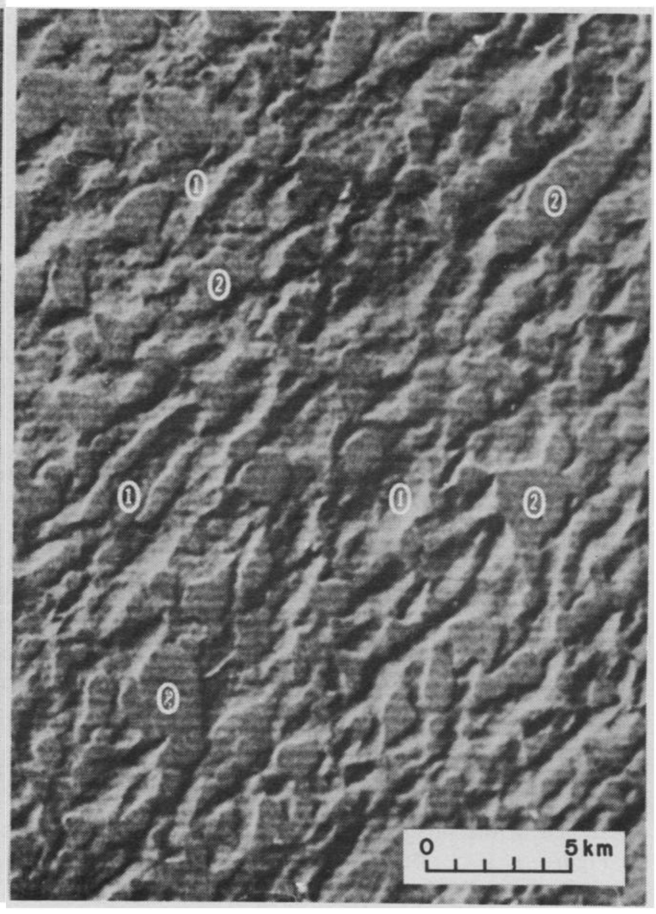

the burial of surface ice or snow by eolian or alluvial deposits (*13*). The fretted terrain (Fig. 1) occurs in an area thought to be composed of volatile-rich, blanket deposits, probably having a large eolian component (*14*). Although terrestrial thermokarsts are significantly smaller in scale than the martian fretted terrain the terrestrial fretted terrain may be significantly older and consequently more well developed. This interpretation is in agreement with that of Sharp (*2*).

Analysis of adjacent ERTS-1 scenes suggests that much of the surface topography on the Alaskan Arctic Coastal Plain is an expression of subsurface structural control of the underlying Cretaceous rocks (*15*). The drainage patterns of most of the major rivers (for example, upper courses of the Colville River, Maybe Creek, Price River, and Kay River) probably reflect underlying structural trends. This is remarkable inasmuch as this underlying structure finds expression through as much as 50 m of overburden. In Fig. 2, one notes that the general alignment of the thermokarsts and undegraded upland areas parallels regional structural trends. In fact, initial degradation of the subsurface ice in this area may have initiated along en echelon minor faults where thermal anomalies were transmitted upward. With continued degradation thermokarst depressions probably became enlarged and began to coalesce. The drainage networks present are undeveloped and insignificant in comparison with the thermokarsts which dominate this setting. Fluvial erosion appears to be inconsequential here in comparison with thermal erosion as the agent responsible for the development of the local relief.

The recognition of this terrestrial analog was possible because of the obliteration of the confusing albedo patterns of standing water and vegetation by snow cover, a low sun angle, and the availability of suitable image enhancement techniques. Success in this area leads one to expect that other terrestrial analogs of martian permafrost terrain will be found. We are presently investigating satellite imagery of the arid Yakutian Lowlands of eastern Siberia where ovoid thermokarst depressions up to 40 m in depth and 5 to 10 km in length have been reported.

LAWRENCE W. GATTO
DUWAYNE M. ANDERSON
U.S. Army Cold Regions Research and Engineering Laboratory, Hanover, New Hampshire 03755

References and Notes

1. The 10 July 1973 issue of the *Journal of Geophysical Research* presents the results of the analysis of Mariner 9 data through 15 November 1972; D. M. Anderson, L. W. Gatto, F. Ugolini, paper presented as part of the North American Contribution to the Second International Permafrost Conference, National Academy of Sciences, Washington, D.C., 1973; R. B. Leighton and B. C. Murray, *Science* **153**, 136 (1966); D. J. Milton, *ibid.* **183**, 654 (1974); D. M. Anderson, E. S. Gaffney, P. F. Low, *ibid.* **155**, 319 (1967); R. B. Leighton, N. H. Horowitz, B. C. Murray, R. P. Sharp, A. H. Herriman, A. T. Young, B. A. Smith, M. E. Davies, C. B. Leovy, *ibid.* **166**, 49 (1969); R. P. Sharp, L. A. Soderblom, B. C. Murray, J. A. Cutts, *J. Geophys. Res.* **76**, 331 (1971).
2. R. P. Sharp, *J. Geophys. Res.* **78**, 4073 (1973).
3. As determined by aerial reconnaissance and reference to U.S. Geological Survey topographic maps.
4. Dr. A. Goetz of the Jet Propulsion Laboratory provided computer time and suggested processing techniques to enhance features of interest. P. Paluzzi of the IPL prepared computer programs, described the processing techniques, and acquired the enhanced photographs. A. Gillespie made several useful suggestions for computer processing. Their assistance is greatly appreciated.
5. J. Dylik, in *Encyclopedia of Geomorphology* (Reinhold, New York, 1968), pp. 1149–1151.
6. F. E. Are, paper presented at the Second International Permafrost Conference, Yakutsk, U.S.S.R., 1973.
7. H. M. French, *Can. J. Earth Sci.* **2**, 785 (1974).
8. R. F. Black, *U.S. Geol. Surv. Prof. Pap. 302-C* (1964), p. 59.
9. T. G. Payne, S. W. Dana, W. A. Fischer, S. T. Yuster, P. D. Krynine, G. Gryc, H. Tappen, R. H. Morris, E. H. Lathram, *U.S. Geol. Surv. Oil Gas Invest. Map OM-126* (1952).
10. J. R. Mackay and R. F. Black, paper presented as part of the North American Contribution to the Second International Permafrost Conference, National Academy of Sciences, Washington, D.C., 1973.
11. R. F. Black, *Biul. Peryglacjalny* **19**, 131 (1969).
12. T. Czudek and J. Demek, *Qualt. Res. (N.Y.)* **1**, 103 (1970).
13. The stratified appearance of some of the martian polar terrain may be caused by similar interlayering.
14. D. U. Wise, personal communication.
15. E. H. Lathram, I. L. Tailleur, W. W. Patton, Jr., *2nd ERTS-1 Symp. Significant Results* **1**, 257 (1973); E. H. Lathram, *3rd ERTS-1 Symp. Significant Results* (1973), p. 39 (abstr.); W. A. Fischer and E. H. Lathram, *Oil Gas J.* **71** (No. 21), 97 (1973).
16. We thank R. P. Sharp, J. A. Cutts, and D. U. Wise for helpful suggestions and for critically reviewing this manuscript during its preparation. This report presents the results of research performed with funds provided by the Planetology Program Office, Office of Space Science, National Aeronautics and Space Administration Headquarters, under grant NGR W-13,277, PR:10-9336,R/D 80X0108(71) 384-50-80.

3 September 1974; revised 24 December 1974

Nitrogen Fixation in a Coral Reef Community

Abstract. *Algal reef flats at Enewetak Atoll, Marshall Islands, fix atmospheric nitrogen at rates comparable to those in managed agriculture. The dominant nitrogen fixer appears to be the blue-green alga* Calothrix crustacea. *Since this nutrient enrichment contributes to the high productivity of adjacent coral reefs and undoubtedly to atoll lagoons, it is recommended that the algal reef flats receive increased conservation priority.*

Coral reef communities are characterized by high rates of biological productivity. The mechanism by which this is accomplished has puzzled marine biologists for years. These communities obtain their nutrients from the overlying waters, and tropical marine waters are generally characterized by low levels of dissolved and particulate nutrients. Fixed nitrogen is in particularly low supply and has been shown to be the major limiting nutrient for phytoplankton production in the tropical Pacific (*1*).

In 1971, during the Symbios expedition to Enewetak Atoll, we observed that the ocean water became markedly enriched with various forms of dissolved and particulate nitrogen as it flowed across a shallow windward interisland reef (*2*). The net rate of nitrogen export was of the order of 3 kg ha^{-1} day^{-0} (*3*). We subsequently found that the source of this localized superabundance of fixed nitrogen was a number of nitrogen-fixing algae, the most abundant and important of which was *Calothrix crustacea* (*4*). Here we describe the role of this species in the nitrogen budget and the biological productivity of Enewetak reef communities.

Calothrix crustacea, a heterocystous blue-green alga, occurs as a thin, yellow-brown, often almost unispecific film covering large portions of the windward intertidal reef flat at Enewetak. At low tide, most of these algae remain moist. During higher stages of the tide, herbivorous reef fish, notably several species of parrotfish and surgeonfish, graze the intertidal reef flat *Calothrix* community. Their tooth marks in the reef rock provide evidence of the thoroughness with which they crop this alga.

Along the upper intertidal bench zone another growth form of the same species occurs as a black, feltlike mat up to 5 mm thick. At low tide, most of this mat dries out. It is not heavily grazed by fish owing to the shallowness of the water in which it grows. In areas of the windward reef flat and outer